Dynamic Multiferroicity of a Ferroelectric Quantum Critical Point

K. Dunnett,[1] J.-X. Zhu,[2] N. A. Spaldin,[3] V. Juričić,[1] and A. V. Balatsky[1,4]
[1]Nordita, KTH Royal Institute of Technology and Stockholm University, Roslagstullsbacken 23, SE-106 91 Stockholm, Sweden
[2]T-4 and CINT, Los Alamos National Laboratory, Los Alamos, New Mexico 87545, USA
[3]Materials Theory, ETH Zurich, Wolfgang-Pauli-Strasse 27, CH-8093 Zürich, Switzerland
[4]Department of Physics, University of Connecticut, Storrs, Connecticut 06269, USA

(Received 17 August 2018; published 8 February 2019)

Quantum matter hosts a large variety of phases, some coexisting, some competing; when two or more orders occur together, they are often entangled and cannot be separated. Dynamical multiferroicity, where fluctuations of electric dipoles lead to magnetization, is an example where the two orders are impossible to disentangle. Here we demonstrate an elevated magnetic response of a ferroelectric near the ferroelectric quantum critical point (FE QCP), since magnetic fluctuations are entangled with ferroelectric fluctuations. We thus suggest that any ferroelectric quantum critical point is an *inherent* multiferroic quantum critical point. We calculate the magnetic susceptibility near the FE QCP and find a region with enhanced magnetic signatures near the FE QCP and controlled by the tuning parameter of the ferroelectric phase. The effect is small but observable—we propose quantum paraelectric strontium titanate as a candidate material where the magnitude of the induced magnetic moments can be $\sim 5 \times 10^{-7}\ \mu_B$ per unit cell near the FE QCP.

DOI: 10.1103/PhysRevLett.122.057208

Quantum matter exhibits a plethora of novel phases and effects upon driving [1], one of which is the strong connection between the quantum critical point (QCP) of one order parameter and the presence of another phase. The discussion has often focused on the relation between superconductivity and one or more magnetic phases [2–4]. However, other fluctuation-driven phase transitions, for example, nematic phases in iron-based superconductors [3,5], have also received significant attention. We focus here on the ferroelectric (FE) QCP which is a key element of the discussion of FE behavior, particularly in displacive quantum paraelectrics [6,7]. The behaviors that may occur near or as a result of such an FE QCP have been explored in various contexts [6–13], and the list of systems where the effects of quantum fluctuations can be observed is expanding, with temperatures up to ~60 K in some organic charge-transfer complexes [10,14].

The concept of dynamical multiferroicity was introduced recently as the dynamical counterpart of the Dzyaloshinskii-Moriya mechanism, reflecting the symmetry between electric and magnetic properties [15]. In the Dzyaloshinskii-Moriya mechanism [16–18], ferroelectric polarization is caused by a spatially varying magnetic structure, leading to strong coupling between ferroelectricity and magnetism [19–21]. In the related phenomenon of dynamical multiferroicity, magnetic moments $\mathbf{m}$ can be induced by time-dependent oscillations of electric dipole moments $\mathbf{p}$:

$$\mathbf{m} = \lambda \mathbf{p} \times \partial_t \mathbf{p} = C \mathbf{n} \times \partial_t \mathbf{n}. \tag{1}$$

For magnetic moments to be induced, $\mathbf{p}$ has to exhibit transverse fluctuations; we therefore focus on rotational degrees of freedom of electric dipole moments [22]. The unit direction vector of the constant amplitude electric dipole moment is $\mathbf{n} \equiv \mathbf{n}(\mathbf{r}, t)$, with time derivative $\partial_t \mathbf{n}$, and $C = \lambda |\mathbf{p}|^2$ in terms of the electric dipole moments $\mathbf{p}$ (we use estimates from uniform polarization $P_0 = |\mathbf{p}| V$ with volume V in FE phases) and coupling $\lambda = \pi / e$, with e the electric charge. Generally, we expect that orders entangled with the underlying static order can be excited dynamically. One possibility is to use external driving mechanisms such as light, a magnetic field, or lattice strain to induce transient excitations of the entangled orders [2]. The present work addresses the complementary case where *inherent* FE quantum fluctuations induce entangled ferromagnetic order fluctuations without any external drive.

In this Letter, we demonstrate the following. (i) The fluctuating dipoles can induce magnetic fluctuations that surround the FE QCP, as shown in Fig. 1(a). The mechanism for this effect is the induction of magnetic moments by fluctuating electric dipoles, described by Eq. (1), near the FE QCP and therefore describes *inherent* dynamic multiferroicity. We support this scenario by calculating the magnetic susceptibility that, as we show, diverges in the paraelectric (PE) phase (Figs. 2 and 3), indicating a transition to a new regime, labeled multiferroic PE in Fig. 1(a). We thus surmise that any FE QCP is a multicritical multiferroic QCP with elevated magnetic fluctuations. We stress that the proposed effect is not due to permanent intrinsic magnetic moments, for example, from unpaired electrons on ions, but arises solely due to the

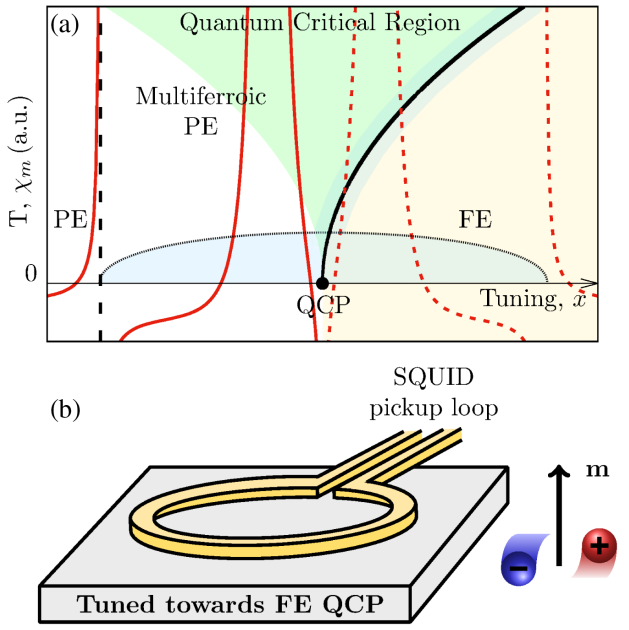

FIG. 1. (a) Phase diagram near a ferroelectric QCP (where $x = x_{cr}$) with the magnetic susceptibility (red line, dashed in the FE phase) at $\omega = 0.5\omega_0$ which diverges at the vertical dashed line, leading to a new "multiferroic PE" phase. The ferroelectric quantum critical region (pale green) is now a dynamical multiferroic quantum critical region. In both the PE (white background) and FE (yellow background) phases, qualitatively similar behaviors of χ_m are expected, despite the different underlying orders. The blue shading indicates the main regions where induced magnetic signatures are expected: a dome around the FE QCP due to quantum fluctuations; a narrow band around the finite temperature phase transition line due to thermally induced fluctuations. (b) A simple experiment using a SQUID could detect magnetic signatures resulting from rotating electric dipoles in a system towards its ferroelectric phase transition. Here, the electric dipoles are constrained to the horizontal plane and lead to an out-of-plane magnetic moment $\mathbf{m}$ and susceptibility.

dynamics of the ferroelectric order. While the proposed effect is general, we consider the specific implications for magnetism in strontium titanate (STO) and provide estimates relevant to STO. (ii) Within the approximations used, the application of a magnetic field $\mathbf{B}$ does not introduce a static, $\mathbf{B}$-dependent mass term to the effective action for $\mathbf{p}$, and the position of the FE QCP is therefore independent of $\mathbf{B}$. The Zeeman splitting of the FE active phonon modes [15,22] meanwhile does affect the magnetic susceptibility χ_m and, in higher-order approximations, is expected to lead to a $\mathbf{B}^2$ term in the free energy, shifting the FE QCP. (iii) We estimate the typical induced magnetic moment from a single rotating electric dipole to be $|\mathbf{m}| \approx 5 \times 10^{-7}\ \mu_B$, where μ_B is the Bohr magneton. This is for coupling $\lambda = \pi/e$ and a dipole with charge $4e$ and length 1×10^{-2} Å, rotating with a frequency of 0.5 THz, typical of the titanium displacements [23–26] and the ferroelectric phonon modes in STO [27–29] (Supplemental Material, Sec. I [30]). The overall contribution of the fluctuating FE order is diamagnetism near the FE QCP.

Model.—The system considered consists of fluctuating electric dipoles close to the PE-FE phase transition, inducing a magnetic moment via Eq. (1). In the absence of external fields, the generic description of the system of rotating electric dipoles consists of the PE phase: $L_{\mathrm{PE}} = (\omega^2 - \omega_q^2)\mathbf{p}_{\omega,q}\mathbf{p}_{-\omega,-q}$, where ω_q is the dispersion of the phonon mode relevant for ferroelectricity and $\mathbf{p}_{\omega,q}$ is the rotating electric dipole moment written in Fourier (energy ω, momentum q) space. The PE phase has a negligible intrinsic magnetic contribution, and we therefore ignore intrinsic magnetization altogether. However, the dynamic induction of $\mathbf{m}$, Eq. (1), will lead to magnetic susceptibility of the paraelectric near the FE QCP.

The interaction between induced magnetic moments can be neglected in the PE phase, since the lowest-order contribution $|\mathbf{m}|^2 \propto |\mathbf{p}|^4$. We assume optical phonons, relevant for the PE-FE transition in STO [27], with dispersion ω_q given by

$$\omega_q^2 = \omega_0^2\left(1 - \frac{x}{x_{cr}}\right) + bq^2 = \omega_0^2\delta_x + bq^2, \qquad (2)$$

where $\delta_x = x/x_{cr}$ describes the distance to the *ferroelectric* QCP at x_{cr}; ω_0 is energy at the zero momentum of the soft mode when $x = 0$, i.e., with no driving of the system towards the FE QCP, and q is the momentum. x is a tuning parameter that controls the PE-FE phase transition at zero temperature, such as doping. If the system is very close to the FE QCP, the momentum dependence is negligible and a flat dispersion with $b = 0$ can be used. The system is paraelectric for $\delta_x > 0$ and ferroelectric when $\delta_x < 0$.

Although in reality both amplitude and directional fluctuations of $\mathbf{p}$ are present near the FE QCP, we will ignore the amplitude fluctuations, so the time dependence of $\mathbf{p}$ is contained entirely in the unit direction vector $\mathbf{n}$. In this model, at the boundary between the PE and FE phases instead of $|\mathbf{p}| \to 0$, the dipoles rotate. That is, in the PE phase, finite-sized electric dipoles are present but not aligned, so the net polarization is zero, and in the FE phase the dipoles align. $\mathbf{n}$ is linearized as $\mathbf{n} = \mathbf{n}_0 + \tilde{\mathbf{n}}(t)$ with $\partial_t \mathbf{n}_0 = 0$ and $\langle\tilde{\mathbf{n}}\rangle = 0$. The zero-temperature Green's function of the $\mathbf{n}$ field in $\omega - q$ space reads

$$\langle\tilde{n}^j_\omega \tilde{n}^m_{-\omega}\rangle = A_j\delta_{jm}G(i\omega, q), \qquad (3)$$

with A_j as a constant factor. To find dynamic susceptibilities, we use the retarded Green's function G^R, obtained by analytical continuation to real frequencies ($i\omega \to \omega + i\eta$, Supplemental Material, Sec. II [30]):

$$G^R(\omega,q) = \mathrm{Re}\left(\frac{1}{\omega_q^2-\omega^2}\right) + \frac{i\pi}{2\omega_q}[\delta(\omega_q-\omega)-\delta(\omega_q+\omega)]. \quad (4)$$

We now calculate the magnetic susceptibility χ_m in the PE phase:

$$\chi_m = \langle \mathbf{m}(r_1,t_1)\mathbf{m}(r_2,t_2)\rangle \equiv \chi^{(1)} + \chi^{(2)}, \quad (5)$$

where $\mathbf{m}$ is given by Eq. (1). The two contributions to χ_m are $\chi^{(1)} \propto \langle \tilde{n}^k \tilde{n}^n \rangle$ and $\chi^{(2)} \propto \langle \tilde{n}^j \tilde{n}^k \tilde{n}^m \tilde{n}^n \rangle$.

The quadratic contribution in $\omega - q$ space is

$$\chi^{(1)}_{il} = C^2 n_0^j n_0^m A_k \epsilon_{ijk}\epsilon_{lmk}\omega^2 G^R(\omega), \quad (6)$$

with $G^R(\omega)$ given by Eq. (4), and the factor $C^2 = \lambda^2 V^4 P_0^4$ gives the size of the magnetic susceptibility in terms of the coupling λ for the induced magnetic moments and the polarization P_0 of a sample of volume V. n_0^i are the components of $\mathbf{n}_0$ around which the fluctuations are expanded. The factor ω^2 comes from the Fourier transform of $\langle \partial_t \tilde{n}^k \partial_t \tilde{n}^n \rangle$.

The quartic contribution to the magnetic susceptibility corresponds to a one-loop diagram as discussed in Supplemental Material, Sec. III [30], with the real part given by

$$\mathrm{Re}[\chi^{(2)}_{ii}] = -\frac{C^2 \delta_{il} A_j A_k \Lambda^3}{8\pi\omega_x} f(\omega), \quad (7)$$

where $f(\omega)$, given in full in Supplemental Material, Sec. III [30], contains δ functions at $2\omega_0\sqrt{\delta_x} \pm \omega$ and ω with weights ω or $\omega_0\sqrt{\delta_x}$, and Λ is a momentum cutoff. The imaginary part is

$$\mathrm{Im}[\chi^{(2)}_{ii}] = \frac{C^2 \delta_{il} A_j A_k \Lambda^3}{\pi^2(\omega^2-4\omega_x^2)}\left(\frac{\omega^2-2\omega_x^2}{2\omega} - \omega_x\right). \quad (8)$$

If the energy ω is written in terms of the $q=0$ phonon energy ω_0, the size of the $\chi^{(2)}$ contribution is determined by Λ^3/ω_0. In STO, areas of coherent fluctuations are limited to tetragonal domains, $\sim 10\ \mu$m [34], in which case $\Lambda^3/\omega_0 \sim 5\times 10^5$, for $\omega_0 = 0.5$ THz, as suitable for the ferroelectric optical phonons in STO. Furthermore, the distribution and size of tetragonal domains can be controlled by both applied electric fields [35,36] and pressure [35].

Results.—The total magnetic susceptibility χ_m from Eq. (5) is plotted in Figs. 2 and 3 with the overall scale given by the shared prefactor $C^2 = \lambda^2 V^4 P_0^4$ set to unity in all plots. In STO samples, the value of C^2 can be estimated from experimental data of samples tuned through the FE phase transition by applied strain or ^{18}O isotope substitution, which indicates the possible size of the dipole moments in the PE phase: $C^2 \sim 2\times 10^{-3}$ C^2 m^4 for bulk STO crystals, and $C^2 \sim 4\times 10^{-34}$ C^2 m^4 for $10\ \mu$m tetragonal domains [23–25]. Considering a sample with a single induced magnetic moment of $5\times 10^{-7}\ \mu_B$ per unit cell and a sample volume of $1\ \mu$m^3, smaller than the tetragonal domains in STO, gives a sample magnetic moment of $8\times 10^4\ \mu_B$, well within spin sensitivities of $200\mu_B/\sqrt{\mathrm{Hz}}$ of current superconducting quantum interference devices (SQUIDs) [37].

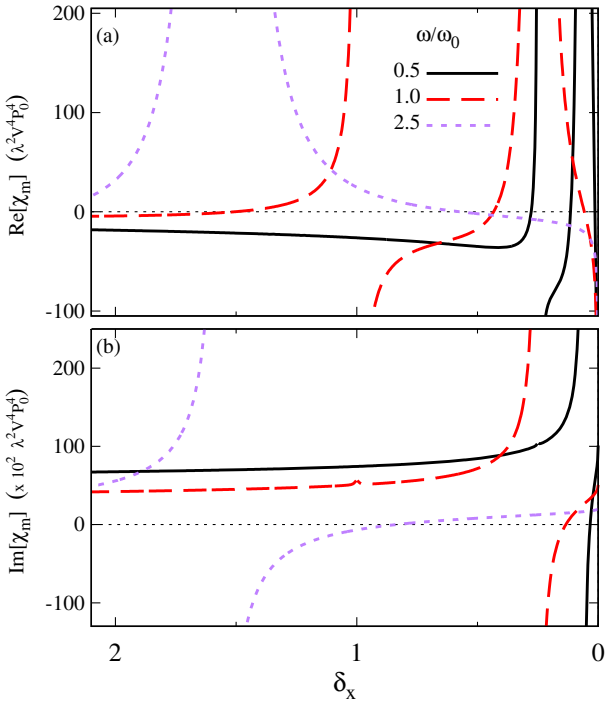

FIG. 2. The total magnetic susceptibility in units of the common prefactor $C^2 = \lambda^2 V^4 P_0^4$, and with $\Lambda^3/\omega_0 = 1\times 10^5$, as a function of δ_x at several energies. (a) The real part; (b) the imaginary part. The behavior in the FE phase $\delta_x < 0$ is expected to share the main qualitative features despite the underlying order. The effects of changing the $\chi^{(2)}$ prefactor Λ^3/ω_0 and the individual contributions of $\chi^{(1)}$ and $\chi^{(2)}$ are discussed in Supplemental Material, Sec. IV [30].

We consider tuning towards the FE QCP at a constant energy (fixed ω/ω_0) first. In Fig. 2(a), far from the FE QCP, the system is dielectric with $\mathrm{Re}[\chi_m] > 0$ but not large. On moving towards the FE QCP, χ_m diverges and changes sign at $\delta_x = (\omega/\omega_0)^2$; this indicates a phase transition into a region where magnetic signatures can be expected. As the energy is decreased, the divergence moves towards the FE QCP, and the magnetic features are confined into a narrower range of the tuning parameter.

There are two contributions to the peaks in the real part of the susceptibility: One is from the poles in $\mathrm{Re}[\chi^{(1)}]$ resulting in the large derivative feature at $\delta_x = (\omega/\omega_0)^2$; the other comes from the δ functions in $\mathrm{Im}[G^R]$ that lead to peaks in $\mathrm{Re}[\chi^{(2)}]$ at $\delta_x = (\omega/2\omega_0)^2$. After the initial divergence, $\mathrm{Re}[\chi_m]$ is negative apart from the sharp

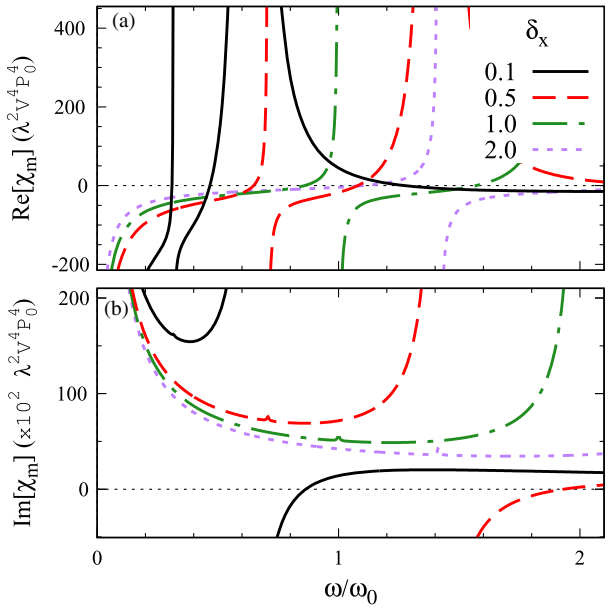

FIG. 3. Total magnetic susceptibility, in units of $C^2 = \lambda^2 V^4 P_0^4$, and with $\Lambda^3/\omega_0 = 1 \times 10^5$, as a function of ω/ω_0 at several distances from the FE QCP. (a) Real part; (b) imaginary part. The peaks in the imaginary part (δ functions plotted as Lorentzian functions) corresponding to the divergence and sign change of the real part are weak for $\Lambda^3/\omega_0 = 1 \times 10^5$ used; their presence is more easily seen at smaller values of Λ^3/ω_0 (Supplemental Material, Sec. IV [30]).

peak at $\delta_x = (\omega/2\omega_0)^2$, below which it quickly reaches a constant negative value independent of ω.

The imaginary part of χ_m, plotted in Fig. 2(b), also diverges as expected at the border of the magnetic region. This is followed by a divergence at $\delta_x = (\omega/2\omega_0)^2$ corresponding to the peaks originating from $\chi^{(2)}$ in the real part. In the limit of $\delta_x \to 0$, $\mathrm{Im}[\chi_m]$ reaches a positive value that depends on the energy ω considered. It is important to note that the details of both the real and imaginary parts once the magnetic phase transition has been passed, that is, for $\delta < (\omega/\omega_0)^2$, are determined solely by the higher-order $\chi^{(2)}$ contributions.

Changing energy while at a fixed distance from the FE QCP is considered in Fig. 3. The peaks and divergences at finite ω correspond to those seen in Fig. 2, with an extra, artificial, divergence of both the real and imaginary parts at $\omega = 0$, originating from calculating $\chi^{(2)}$ in the continuum limit. At the lowest energies, $\mathrm{Re}[\chi_m] < 0$, it then increases and diverges at $\omega/\omega_0 = \sqrt{\delta_x}$, thus signaling the phase transition with magnetic signatures expected above a critical energy scale. We note that, upon increasing δ_x to move away from the QCP, the onset of the transition moves to a higher energy. The energy dependence of the size of the imaginary part is seen particularly clearly in Fig. 3(b). In the FE phase, we expect qualitatively similar features, despite the underlying FE order, due to fluctuations of the ordered dipoles.

A magnetic field $\mathbf{B}$, applied perpendicular to the plane of the rotating dipoles, will have two effects. First, the phonon Zeeman effect splits the phonon modes with a linear dependence on $\mathbf{B}$ [15] and moves the divergence of χ_m [which occurs at $\delta = (\omega/\omega_0)^2$ for $\mathbf{B} = 0$]. Second, an additional term in the Lagrangian for the interaction of the induced magnetic moments with the $\mathbf{B}$, $\mathbf{B} \cdot \mathbf{m} = \lambda \mathbf{B} \cdot (\mathbf{p} \times \partial_t \mathbf{p})$ [22], can be treated as a perturbation to the paraelectric system. Calculating the corresponding second-order diagram (Supplemental Material, Sec. V [30]) does not introduce a static, $\mathbf{B}$-dependent mass term but may do so at higher orders.

Experimental proposal.—STO may be a suitable candidate material for the observation of magnetic signatures on tuning towards the FE QCP because of its incipient ferroelectric nature below ~35 K and its quantum paraelectric nature below 4 K [38], where the zero-point motion of the soft transverse optical phonon mode is high enough to prevent ferroelectricity even at a zero temperature [39]. In ^{18}O-substituted STO, $\omega_{q=0}(T)$ becomes constant below 4–10 K depending on the distance from the FE QCP [40–44]. Thus, rotating electric dipoles could be present over an appreciable temperature range. Additional flexibility exists, because several methods are available for tuning STO towards the FE QCP, such as Ca doping [45], ^{18}O substitution [24,25,46], strain, or applied pressure [23,28].

A simple experimental setup, consisting of a SQUID above an STO sample, that may permit the observation of the region of pronounced magnetic fluctuations is sketched in Fig. 1(b). Strain is a particularly flexible means of tuning STO samples towards the FE QCP, and biaxial strain in STO thin films can confine polarization to the plane perpendicular to the tetragonal c axis but does not unambiguously determine the polarization direction [47–50], a favorable condition for the observation of the magnetic signatures proposed here. Although strained STO is considered here, other FE QCPs and tuning mechanisms could be studied, e.g., $Ca_{1-x}Pb_xTiO_3$ [51] and strained $KTaO_3$ [52]. The quantum dipole phase of the triangular lattice Mott insulator κ-$(BEDT\text{-}TTF)_2Hg(SCN)_2Br$ [53] may also exhibit magnetic signatures of inherent dynamical multiferroicity. The crucial ingredient for inherent dynamical multiferroicity is incipient ferroelectricity (or quantum paraelectricity) and only weak anisotropy between at least two in-plane polarization directions, to allow the fluctuations to well-defined circulating ions.

Discussion.—Including the long-range interactions between electric dipoles, such as those resulting from twin boundaries between tetragonal domains with differently oriented c axes [54,55], would introduce off-diagonal terms to the Green's function [50]. The immediate effect is a nonzero average magnetization $\langle \mathbf{M} \rangle \propto \langle \mathbf{n} \times \partial_t \mathbf{n} \rangle$. Alongside this, the off-diagonal components of the dielectric susceptibility $\chi_e^{ij} = \langle p_i p_j \rangle \propto \langle \tilde{n}^i \tilde{n}^j \rangle$ would also be nonzero at

the twin boundaries, leading to a finite Kerr effect [56]. Furthermore, the motion of twin boundaries may be a means to induce relevant fluctuations of the electric dipoles [57]. Scanning SQUID measurements able to resolve the individual tetragonal domains would be required to investigate the effects of domain structures on the magnetic signals. Again, STO is a potential candidate material, since tetragonal domains form naturally on cooling through the antiferrodistortive structural phase transition at 105 K and their distribution can be controlled by applied pressure [35].

The situation examined here is distinct from that recently considered in the context of multiferroic criticality [12] and other systems where the quantum critical points of two or more types of order can be tuned by the same or different parameters leading to a fan where the quantum fluctuations of both orders are important [12,58]. In our model, the magnetic order does not exist independently of the ferroelectric order, leading to an FE quantum critical region that is surrounded by a region of strong magnetic fluctuations. While distinct from the nematic phase transitions seen in iron pnictides [5,59], the multiferroic paraelectric region is another realization of competing orders near a QCP. The interaction between the induced magnetic moments and an external magnetic field is expected to mostly affect the nature of the FE phase transition, as discussed for magnetic phase transitions [60–62].

Conclusions.—We have expanded the framework of dynamic multiferroicity [15] and predict strongly enhanced ferromagnetic (FM) susceptibility in a paraelectric material near its FE QCP. The induced magnetic susceptibility diverges at a finite distance from the FE QCP. The predicted effect indicates another way for entangled quantum orders to appear. On the approach to the FE QCP, the fluctuations of the entangled (FM) order are enhanced as the static FE order develops quantum fluctuations. We thus suggest that any FE QCP may be an *inherent* multiferroic QCP with entangled ferroelectric and (much weaker but present) ferromagnetic fluctuations. We expect magnetic signatures of fluctuating dipoles to be observable experimentally, e.g., in SQUID measurements, and could lead to additional signatures in optical Kerr and Faraday effects. Our results are applicable to any ferroelectric-paraelectric transition including classical transitions at finite temperatures, where the fluctuations will be confined to a narrow Ginzburg-Levanyuk region near the transition. The effect will become pronounced near the $T = 0$ QCP. Finally, to illustrate this scenario, we have considered STO as a system that can be tuned towards its FE QCP.

We are grateful to G. Aeppli, J. Lashley, and I. Sochnikov for useful discussions. The work was supported by the U.S. Department of Energy BES E3B7, by VILLUM FONDEN via the Centre of Excellence for Dirac Materials (Grant No. 11744), and by The Knut and Alice Wallenberg Foundation (2013.0096).

[1] D. N. Basov, D. A. Averitt, and D. Hsieh, Towards properties on demand in quantum materials, Nat. Mater. **16**, 1077 (2017).
[2] P. Gegenwart, Q. Si, and F. Steglich, Quantum criticality in heavy-fermion metals, Nat. Phys. **4**, 186 (2008).
[3] T. Shibauchi, A. Carrington, and Y. Matsuda, A quantum critical point lying beneath the superconducting dome in iron pnictides, Annu. Rev. Condens. Matter Phys. **5**, 113 (2014).
[4] C. M. Varma, Quantum-critical fluctuations in 2D metals: Strange metals and superconductivity in antiferromagnets and in cuprates, Rep. Prog. Phys. **79**, 082501 (2016).
[5] R. M. Fernandes, A. V. Chubukov, and J. Schmalian, What drives nematic order in iron-based superconductors?, Nat. Phys. **10**, 97 (2014).
[6] S. E. Rowley, L. J. Spalek, R. P. Smith, M. P. M. Dean, M. Itoh, J. F. Scott, G. G. Lonzarich, and S. S. Saxena, Ferroelectric quantum criticality, Nat. Phys. **10**, 367 (2014).
[7] P. Chandra, G. G. Lonzarich, S. E. Rowley, and J. F. Scott, Prospects and applications near ferroelectric quantum phase transitions: a key issues review, Rep. Prog. Phys. **80**, 112502 (2017).
[8] L. Pálová, P. Chandra, and P. Coleman, Quantum critical paraelectrics and the Casimir effect in time, Phys. Rev. B **79**, 075101 (2009).
[9] J. M. Edge, Y. Kedem, U. Aschauer, N. A. Spaldin, and A. V. Balatsky, Quantum Critical Origin of the Superconducting Dome in $SrTiO_3$, Phys. Rev. Lett. **115**, 247002 (2015).
[10] S. Rowley, M. Hadjimichael, M. N. Ali, Y. C. Durmaz, J. C. Lashley, R. J. Cava, and J. F. Scott, Quantum criticality in a uniaxial organic ferroelectric, J. Phys. Condens. Matter **27**, 395901 (2015).
[11] C. W. Rischau, X. Lin, C. P. Grams, D. Finck, S. Hams, J. Engelmayer, T. Lorenz, Y. Gallais, B. Fauqué, J. Hemberger, and K. Behnia, A ferroelectric quantum phase transition inside the superconducting dome of $Sr_{1-x}Ca_xTiO_{3-\delta}$, Nat. Phys. **13**, 643 (2017).
[12] A. Narayan, A. Cano, A. V. Balatsky, and N. A. Spaldin, Multiferroic quantum criticality, Nat. Mater., DOI: 10.1038/s41563-018-0255-6 (2018).
[13] J. Arce-Gamboa and G. Guzmán-Verri, Quantum ferroelectric instabilities in superconducting $SrTiO_3$, Phys. Rev. Mater. **2**, 104804 (2018).
[14] S. Horiuchi, K. Kobayashi, R. Kumai, N. Minami, F. Kagawa, and Y. Tokura, Quantum ferroelectricity in charge-transfer complex crystals, Nat. Commun. **6**, 7469 (2015).
[15] D. M. Juraschek, M. Fechner, A. V. Balatsky, and N. A. Spaldin, Dynamical multiferroicity, Phys. Rev. Mater. **1**, 014401 (2017).
[16] I. Dzyaloshinsky, A thermodynamic theory of "weak" ferromagnetism of antiferromagnetics, J. Phys. Chem. Solids **4**, 241 (1958).
[17] T. Moriya, New Mechanism of Anisotropic Superexchange Interaction, Phys. Rev. Lett. **4**, 228 (1960).
[18] T. Moriya, Anisotropic superexchange interaction and weak ferromagnetism, Phys. Rev. **120**, 91 (1960).
[19] H. Katsura, N. Nagaosa, and A. V. Balatsky, Spin Current and Magnetoelectric Effect in Noncollinear Magnets, Phys. Rev. Lett. **95**, 057205 (2005).

[20] I. A. Sergienko and E. Dagotto, Role of the Dzyaloshinskii-Moriya interaction in multiferroic perovskites, Phys. Rev. B **73**, 094434 (2006).

[21] S.-W. Cheong and M. Mostovoy, Multiferroics: A magnetic twist for ferroelectricity, Nat. Mater. **6**, 13 (2007).

[22] I. E. Dzyaloshinskii and D. L. Mills, Intrinsic paramagnetism of ferroelectrics, Philos. Mag. **89**, 2079 (2009).

[23] W. J. Burke and R. J. Pressley, Stress induced ferroelectricity in $SrTiO_3$, Solid State Commun. **9**, 191 (1971).

[24] M. Itoh, R. Wang, Y. Inaguma, T. Yamaguchi, Y.-J. Shan, and T. Nakamura, Ferroelectricity Induced by Oxygen Isotope Exchange in Strontium Titanate Perovskite, Phys. Rev. Lett. **82**, 3540 (1999).

[25] R. Wang and M. Itoh, Suppression of the quantum fluctuation in ^{18}O-enriched strontium titanate, Phys. Rev. B **64**, 174104 (2001).

[26] W. A. Atkinson, P. Lafleur, and A. Raslan, Influence of the ferroelectric quantum critical point on $SrTiO_3$ interfaces, Phys. Rev. B **95**, 054107 (2017).

[27] Y. Yamada and G. Shirane, Neutron scattering and nature of the soft optical phonon in $SrTiO_3$, J. Phys. Soc. Jpn. **26**, 396 (1969).

[28] H. Uwe and T. Sakudo, Stress-induced ferroelectricity and soft phonon modes in $SrTiO_3$, Phys. Rev. B **13**, 271 (1976).

[29] A. Yamanaka, M. Kataoka, Y. Inaba, K. Inoue, B. Hehlen, and E. Courtens, Evidence for competing orderings in strontium titanate from hyper-Raman scattering spectroscopy, Europhys. Lett. **50**, 688 (2000).

[30] See Supplemental Material at http://link.aps.org/supplemental/10.1103/PhysRevLett.122.057208 for further details, which contains additional Refs. [31–33].

[31] D. J. Griffiths, *Introduction to Electrodynamics*, 3rd ed. (Pearson Benjamin Cummings, San Francisco, 2008).

[32] G. D. Mahan, *Many-Particle Physics*, Physics of Solids and Liquids, 2nd ed. (Plenum, New York, 1990).

[33] R. H. White, *Quantum Theory of Magnetism*, Springer Series in Solid-State Sciences (Springer, Berlin, 2007), Vol. 32.

[34] H. Noad, E. M. Spanton, K. C. Nowack, H. Inoue, M. Kim, T. A. Merz, C. Bell, Y. Hikita, R. Xu, W. Liu, A. Vailionis, H. Y. Hwang, and K. A. Moler, Variation in superconducting transition temperature due to tetragonal domains in two-dimensionally doped $SrTiO_3$, Phys. Rev. B **94**, 174516 (2016).

[35] J. Hemberger, M. Nicklas, R. Viana, P. Lunkenheimer, A. Loidl, and R. Böhmer, Quantum paraelectric and induced ferroelectric states in $SrTiO_3$, J. Phys. Condens. Matter **8**, 4673 (1996).

[36] M. Honig, J. A. Sulpizio, J. Drori, A. Joshua, E. Zeldov, and S. Ilani, Local electrostatic imaging of striped domain order in $LaAlO_3/SrTiO_3$, Nat. Mater. **12**, 1112 (2013).

[37] M. E. Huber, N. C. Koshnick, H. Bluhm, L. J. Archuleta, T. Azua, P. G. Bjrnsson, B. W. Gardner, S. T. Halloran, E. A. Lucero, and K. A. Moler, Gradiometric micro-SQUID susceptometer for scanning measurements of mesoscopic samples, Rev. Sci. Instrum. **79**, 053704 (2008).

[38] K. A. Müller and H. Burkard, $SrTiO_3$: An intrinsic quantum paraelectric below 4 K, Phys. Rev. B **19**, 3593 (1979).

[39] E. Courtens, B. Hehlen, G. Coddens, and B. Hennion, New excitations in quantum paraelectrics, Physica (Amsterdam) **219B–220B**, 577 (1996).

[40] H. Vogt, Refined treatment of the model of linearly coupled anharmonic oscillators and its application to the temperature dependence of the zone-center soft-mode frequencies of $KTaO_3$ and $SrTiO_3$, Phys. Rev. B **51**, 8046 (1995).

[41] Y. Yamada, N. Todoroki, and S. Miyashita, Theory of ferroelectric phase transition in $SrTiO_3$ induced by isotope replacement, Phys. Rev. B **69**, 024103 (2004).

[42] M. Takesada, M. Itoh, and T. Yagi, Perfect Softening of the Ferroelectric Mode in the Isotope-Exchanged Strontium Titanate of $SrTi^{18}O_3$ Studied by Light Scattering, Phys. Rev. Lett. **96**, 227602 (2006).

[43] H. Taniguchi, M. Itoh, and T. Yagi, Ideal Soft Mode-Type Quantum Phase Transition and Phase Coexistence at Quantum Critical Point in ^{18}O-Exchanged $SrTiO_3$, Phys. Rev. Lett. **99**, 017602 (2007).

[44] S. E. M. Tchouobiap, A theoretical study of soft mode behavior and ferroelectric phase transition in 18O-isotope exchanged $SrTiO_3$: evidence of phase coexistence at the quantum critical point, Phys. Scr. **89**, 025702 (2014).

[45] J. G. Bednorz and K. A. Müller, $Sr_{1-x}Ca_xTiO_3$: An XY Quantum Ferroelectric with Transition to Randomness, Phys. Rev. Lett. **52**, 2289 (1984).

[46] M. Itoh and R. Wang, Quantum ferroelectricity in $SrTiO_3$ induced by oxygen isotope exchange, Appl. Phys. Lett. **76**, 221 (2000).

[47] N. A. Pertsev, A. K. Tagantsev, and N. Setter, Phase transitions and strain-induced ferroelectricity in $SrTiO_3$ epitaxial thin films, Phys. Rev. B **61**, R825 (2000).

[48] L. Ni, Y. Liu, C. Song, W. Wang, G. Han, and Y. Ge, First-principle study of strain-driven phase transition in incipient ferroelectric $SrTiO_3$, Physica (Amsterdam) **406B**, 4145 (2011).

[49] F. Sun, H. Khassaf, and S. P. Alpay, Strain engineering of piezoelectric properties of strontium titanate thin films, J. Mater. Sci. **49**, 5978 (2014).

[50] R. Roussev and A. J. Millis, Theory of the quantum paraelectric-ferroelectric transition, Phys. Rev. B **67**, 014105 (2003).

[51] V. V. Lemanov, A. V. Sotnikov, E. P. Smirnova, and M. Weihnacht, From incipient ferroelectricity in $CaTiO_3$ to real ferroelectricity in $Ca_{1-x}Pb_xTiO_3$ solid solutions, Appl. Phys. Lett. **81**, 886 (2002).

[52] M. Tyunina, J. Narkilahti, M. Plekh, R. Oja, R. M. Nieminen, A. Dejneka, and V. Trepakov, Evidence for Strain-Induced Ferroelectric Order in Epitaxial Thin-Film $KTaO_3$, Phys. Rev. Lett. **104**, 227601 (2010).

[53] N. Hassan, S. Cunningham, M. Mourigal, E. I. Zhilyaeva, S. A. Torunova, R. N. Lyubovskaya, J. A. Schlueter, and N. Drichko, Evidence for a quantum dipole liquid state in an organic quasi-two-dimensional material, Science **360**, 1101 (2018).

[54] H. J. Harsan Ma, S. Scharinger, S. W. Zeng, D. Kohlberger, M. Lange, A. Stöhr, X. Renshaw Wang, T. Venkatesan, R. Kleiner, J. F. Scott, J. M. D. Coey, D. Koelle, and Ariando, Local Electrical Imaging of Tetragonal Domains and Field-Induced Ferroelectric Twin Walls in Conducting $SrTiO_3$, Phys. Rev. Lett. **116**, 257601 (2016).

[55] Y. Frenkel, N. Haham, Y. Shperber, C. Bell, Y. Xie, Z. Chen, Y. Hikita, H. Y. Hwang, E. K. H. Salje, and B. Kalisky,

Imaging and tuning polarity at $SrTiO_3$ domain walls, Nat. Mater. **16**, 1203 (2017).

[56] B. Gu, S. Takahashi, and S. Maekawa, Enhanced magneto-optical Kerr effect at Fe/insulator interfaces, Phys. Rev. B **96**, 214423 (2017).

[57] R. T. Brierley and P. B. Littlewood, Domain wall fluctuations in ferroelectrics coupled to strain, Phys. Rev. B **89**, 184104 (2014).

[58] C. Morice, P. Chandra, S. E. Rowley, G. Lonzarich, and S. S. Saxena, Hidden fluctuations close to a quantum bicritical point, Phys. Rev. B **96**, 245104 (2017).

[59] R. M. Fernandes, A. V. Chubukov, J. Knolle, I. Eremin, and J. Schmalian, Preemptive nematic order, pseudogap, and orbital order in the iron pnictides, Phys. Rev. B **85**, 024534 (2012).

[60] J.-H. She, J. Zaanen, A. R. Bishop, and A. V. Balatsky, Stability of quantum critical points in the presence of competing orders, Phys. Rev. B **82**, 165128 (2010).

[61] U. Karahasanovic, F. Krüger, and A. G. Green, Quantum order-by-disorder driven phase reconstruction in the vicinity of ferromagnetic quantum critical points, Phys. Rev. B **85**, 165111 (2012).

[62] B. Liu and J. Hu, Quantum fluctuation-driven first-order phase transitions in optical lattices, Phys. Rev. A **92**, 013606 (2015).